Speckle intensity images of target based on Monte Carlo method*

Wu Ying-Li(武颖丽)† and Wu Zhen-Sen(吴振森)

Xidian University, School of Science, Xi'an 710071, *China*

(Received 2 May 2013; revised manuscript received 3 August 2013; published online 12 February 2014)

Speckle intensity in the detector plane is deduced in the free-space optical system and imaging system based on Van Cittert–Zernike theorem. The speckle intensity images of plane target and conical target are obtained by using the Monte Carlo method and measured experimentally. The results show that when the range extent of target is smaller, the speckle size along the same direction become longer, and the speckle size increase with increasing incident light wavelengths. The speckle size increases and the speckle intensity images of target is closer to the actual object when the aperture scale augments. These findings are useful to access the target information by speckle in laser radar systems.

Keywords: laser scattering, Monte Carlo method, speckle, intensity images

PACS: 78.20.hc, 78.20.Ek, 78.20.Bh, 78.68.+m **DOI:** 10.1088/1674-1056/23/3/037801

1. Introduction

According to the principle of information processing in a laser radar, the scattering signal from a diffuse target consists of two parts: a coherent component and a non-coherent component which is a reason that laser speckle forms. The intensity distribution of a speckle pattern and the interference of backscattered light from various scattering points on objects can help us to determine the three-dimensional (3D) characteristics of the object. Hence, laser speckle techniques were motivated by the application of laser radar to target discrimination in ballistic missile defence, and also have shifted to industrial applications of 3D imaging involving machine vision and dimensional metrology.

The performance of an imaging technique relying on the spatial correlation of laser-speckle intensity measurements is evaluated on the basis of theoretical analysis, computer simulation, and experimental results by David in 1991.[1] In 1997, he presented an approach for simulating the effects that partial temporal coherent illumination has on these techniques which are coherent imaging techniques relying on the coherence properties of backscattered radiation to form an image of an illuminated object.[2]

Advanced ladar signal simulator (ALASS) (Lockheed Martin, 2008) is a comprehensive laser radar simulator that synthesizes radar signals for complex 3D dynamic diffuse targets. ALASS provides single realization speckle random signals or associated mean signals of ensemble rough target average, and it is radiometrically correct, accurately models receiver diffraction and defocus for both coherent and direct detection transceivers with single or multi-element detectors, and generates signals with correct 3D speckle statistics.[3] The Swedish Defense Research Agency-FOI give a model that general direct-detection laser radar system applicable for hard target measurements, and derive the time and range dependent laser radar cross sections for some simple geometric shapes (plane, cone, sphere, and parabola). They found the proper statistical distribution of uncertainty in time-of-flight range estimations using the cross section models in simulations.[4,5] In 2010, Song extracted the real and imaginary parts of the complex amplitudes of the speckle in a large angle scattering, and found that the speckle has a property of regional factuality by calculating the spatial correlation functions of intensity.[6] Liu studied the femtosecond temporal speckle field arising from the interference of multiple randomly scattered electric fields by using theory and experiment.[7] In 2013, Zeng *et al.* presented a method of intensity fluctuation modulation to obtain a full-field laser speckle micro vessel image.[8] Feng *et al.* proposed a laser speckle projection tomography method to obtain a three-dimensional flowing image.[9]

In this paper, we simulate the speckle intensity images of plane target and conical target with the Van Cittert–Zernike theorem, analyze the impact on wavelengths, aperture and detection range on it.

2. Scattering strength of target distribution

According to the Van Cittert–Zernike theorem, properties of speckle on the observation plane are correlated with the distribution of target scattering strength, rather than the scattering characteristics of an object. Figure 1 illustrates the beams propagating in free space under paraxial approximation. The

*Project supported by the National Natural Sciences Foundation of China (Grant No. 61172031) and the Fundamental Research Funds for the Central Universities of China (Grant No. K50511070005).

†Corresponding author. E-mail: ylwu@xidian.edu.cn

© 2014 Chinese Physical Society and IOP Publishing Ltd

mutual intensity at the observation plane can be given by[10]

$$J_i(x_i,y_i;x_i',y_i') = \frac{1}{(\lambda z)^2}\iint_{\infty}\iint J_o(x_o,y_o;x_o',y_o') \times \exp\left[-j\frac{2\pi}{\lambda}(r_2-r_1)\right]\mathrm{d}x_o\mathrm{d}y_o\mathrm{d}x_o'\mathrm{d}y_o'. \quad (1)$$

Let L_s be the biggest linear scale of the scattered target and L_c be the biggest correlation linear scale of scattered fields. In terms of $z > 4\overline{x_o}\Delta x_o/\lambda$, $z > 4\overline{y_o}\Delta y_o/\lambda$, and $z > 2L_sL_c/\lambda$, equation (1) takes the form of

$$J_i(x_i,y_i;x_i',y_i') = \frac{\kappa(\overline{x_i},\overline{y_i})\exp[-\mathrm{j}\psi]}{(\lambda z)^2} \times \iint_{\infty} I(\overline{x_o},\overline{y_o})\exp\left[\mathrm{j}\frac{2\pi}{\lambda z}(\Delta x_i\overline{x_o}+\Delta y_i\overline{y_o})\right] \times \mathrm{d}\overline{x_o}\mathrm{d}\overline{y_o}, \quad (2)$$

$$\kappa(\overline{x_i},\overline{y_i}) = \iint_{\infty}\mu(\Delta x_o,\Delta y_o)\exp\left[\mathrm{j}\frac{2\pi}{\lambda z}(\overline{x_i}\Delta x_o+\overline{y_i}\Delta y_o)\right] \times \mathrm{d}\Delta x_o\mathrm{d}\Delta y_o, \quad (3)$$

where $\psi = (2\pi/\lambda z)(\overline{x_i}\Delta x_i+\overline{y_i}\Delta y_i)$, $\overline{x_i} = (x_i+x_i')/2$, $\overline{y_i} = (y_i+y_i')/2$, $I(\overline{x_o},\overline{y_o})$ is the intensity distribution of the object's surface, and the Fourier transform of $I(\overline{x_o},\overline{y_o})$ reflects the correlation between two points Δx_i, Δy_i. The average strength of the scattered field is given by

$$I_i(x_i,y_i) = \frac{\iint_{\infty} I(\overline{x_o},\overline{y_o})\mathrm{d}\overline{x_o}\mathrm{d}\overline{y_o}}{(\lambda z)^2} \times \iint_{\infty}\mu(\Delta x_o,\Delta y_o)\exp\left[j\frac{2\pi}{\lambda z}(x_i\Delta x_o+y_i\Delta y_o)\right] \times \mathrm{d}\Delta x_o\mathrm{d}\Delta y_o. \quad (4)$$

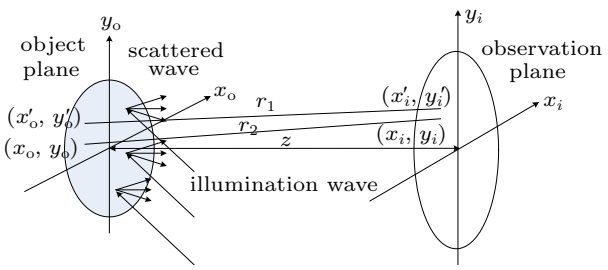


Fig. 1. Propagation of beams in free space.

3. Speckle intensity images of plane target

For a rectangle diffuse target with lengths of L_x and L_y, the intensity uniform distribution is given by

$$I(x_o,y_o) = I_o\mathrm{rect}\left(\frac{x_o}{L_x}\right)\mathrm{rect}\left(\frac{y_o}{L_y}\right). \quad (5)$$

The relevant function of the intensity is expressed as

$$\Gamma_I(\Delta x_i,\Delta y_i) = \bar{I}^2\left[1+|\mu(\Delta x_i,\Delta y_i)|^2\right], \quad (6)$$

where $\mu(\Delta x_i,\Delta y_i) = J_i(\Delta x_i,\Delta y_i)/J_i(0,0)$. The scattering field at the receiver is

$$\Gamma_I(\Delta x_i,\Delta y_i) = \bar{I}^2\left[1+\mathrm{sin}c^2\left(\frac{L_x\Delta x_i}{\lambda z}\right)\mathrm{sin}c^2\left(\frac{L_y\Delta y_i}{\lambda z}\right)\right]. \quad (7)$$

The spectral density is

$$F(\nu_X,\nu_Y) = \bar{I}^2\left[\delta(\nu_X,\nu_Y)+\frac{(\lambda z)^2}{A}\Lambda\left(\frac{\lambda z}{L_x}\nu_X\right)\Lambda\left(\frac{\lambda z}{L_y}\nu_Y\right)\right], \quad (8)$$

where

$$\Lambda(x) = \begin{cases}1-|x|, & |x|\le 0,\\ 0, & \text{otherwise},\end{cases}$$

and $A = L_xL_y$. First, the zero of function $\mathrm{sin}c$ in Eq. (7) is the average speckle size $d = \lambda z/L_x$ along the x direction and $d = \lambda z/L_x$ along the y direction. This relation shows that speckle size is proportional to the distance z but inversely proportional to the range of direction. Figure 2 shows the speckle intensity image on the observation plane though free space by the Monte Carlo method. For the sake of convenient comparison, the observation plane has a size of 136 mm × 136 mm.

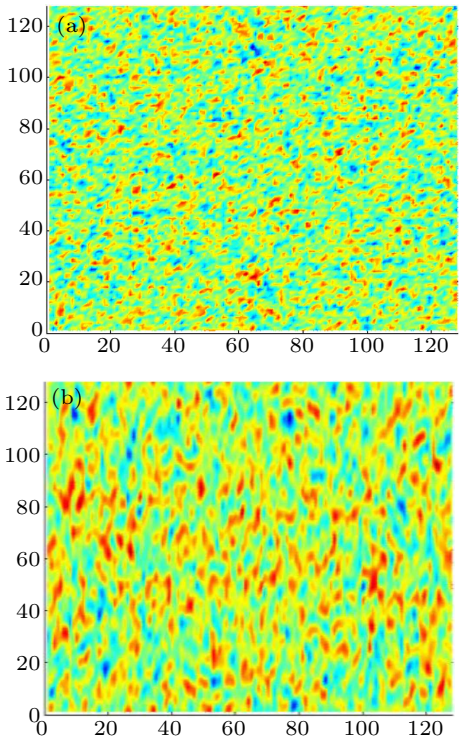


Fig. 2. (color online) Speckle intensity image of plane with different size uniform irradiation. (a) $L_x = 1$ cm, $L_y = 1$ cm; (b) $L_x = 1$ cm, $L_y = 0.3$ cm.

In Fig. 2(a), $L_x = L_y = 1$ cm, $\lambda = 1.06$ μm, $z = 1$ m, and $d = 1.06$ mm. The difference in Fig. 2(b) from Fig. 2(a) is $L_y = 0.3$ cm. It is shown that the speckle size in y direction is larger than that in Fig. 2(a). In Fig. 3(a), $L_x = L_y = 1$ cm, λ =532 nm, and the distance between the scattering plane and observed plane $z = 2$ m. The speckle size in this case is the double of speckle size in Fig. 2(a) since the incident wavelength is the half of Fig. 2(a). Furthermore, figure 3(b) is for the case of $L_x = L_y = 1$ cm and $z = 1$ m. Speckle size is smaller than that of Fig. 3(a), because of the variable z.

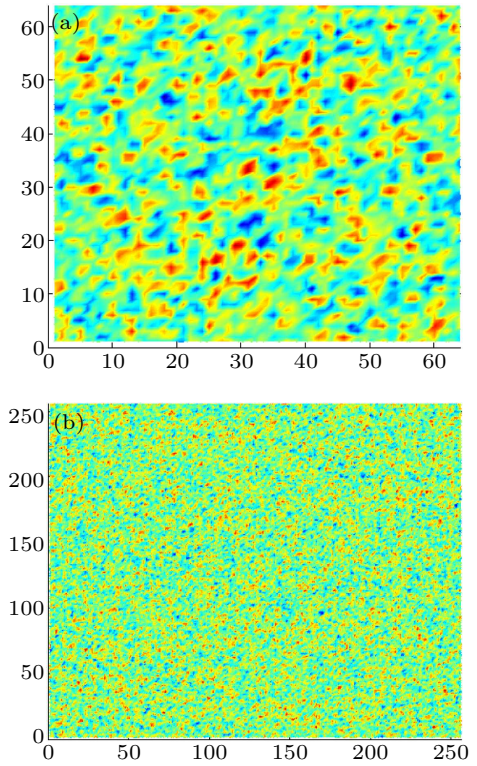


Fig. 3. (color online) Effect of (a) distance and (b) wavelengths on the speckle image of plane.

4. Speckle intensity images of cone target

4.1. Strength distribution of the scattered field from cone

Figure 4 shows the schematic of speckle in space imaging. As the scattering field from rough surface is a random field, distribution of this magnitude and phase can be seen as a random process.

In the quasi-monochromatic approximation, $u_o(x_o,y_o)$ represents the scattered field of the plane near the target, and $u_i(x_i,y_i)$ is the field in the imaging plane. Then mutual intensity of the image plane is

$$J_i(x_i,y_i;x_i',y_i') = \Big\langle \iint_{\infty} u_o(x_o,y_o)h(x_i,y_i;x_o,y_o)\,\mathrm{d}x_o\,\mathrm{d}y_o \times \iint_{\infty} u_o^*(x_o',y_o')h^*(x_i',y_i';x_o',y_o')\,\mathrm{d}x_o'\,\mathrm{d}y_o'\Big\rangle, \quad (9)$$

where h is the impulse response of in-space imaging without the complex phase, and is given by

$$h(x_i,y_i;x_o,y_o) \approx \frac{1}{\lambda^2 z_i z_o}\iint_{\infty} P(x,y)\exp\Big\{-j\frac{2\pi}{\lambda z_i}((x_i-Mx_o)x + (y_i-My_o)y)\Big\}\mathrm{d}x\mathrm{d}y, \quad (10)$$

where $M=-z_i/z_o$ is the transverse magnifying rate, and $P(x,y)$ is the aperture function. When the incident wave is a complete coherent light, the intensity is

$$I_i(x_i,y_i) = \Big|\iint_{\infty} A(x_o,y_o)h(x_i,y_i;x_o,y_o)\,\mathrm{d}x_o\,\mathrm{d}y_o\Big|^2, \quad (11)$$

where $A(x_o,y_o)$ is complex amplitude field distribution and $|A(x_o,y_o)|^2 = I_o(x_o,y_o)$. The mutual intensity of diffuse target scattering surface is

$$I_o(x_o,y_o) = |s_c(\overline{\rho})|^2 I_{inc}(x_o,y_o), \quad (12)$$

where $s_c(\overline{\rho})$ is the complex scattering coefficient and $\langle s_c(\overline{\rho})s_c^*(\overline{\rho}')\rangle = \rho_\pi\delta(\overline{\rho}-\overline{\rho}')$ for the Lambertian surface, $\overline{\rho}$ is the two-dimensional coordinate space and abandoned represents the target's, but no abandoned represent the detector's. In addition, $\rho_\pi = (\rho/\pi)\cos(\theta_s)$, ρ is the diffusing reflectance of the surface material, and θ_s is the angle between the normal of the surface area and the sight of detector.

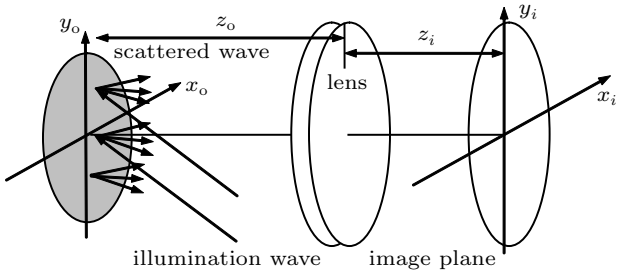


Fig. 4. Schematic of subjective speckle.

4.2. Simulation of cone's speckle intensity images

In the following, we emulate speckle intensity images of the target by the Monte Carlo method (Eq. (12)).

At first, the incident field can be represented by $m\times n$ grid data and each point represents a speckle intensity. We define the incident light intensity matrix as

$$\boldsymbol{I}_{incMN} = \begin{pmatrix} I_{1,1} & \cdots & I_{1,n} \\ \vdots & \ddots & \vdots \\ I_{n,1} & \cdots & I_{n,n} \end{pmatrix}. \quad (13)$$

The scattering intensity matrix can be obtained by multiplying Eq. (13) by ρ_π, the amplitude matrix can gain by further each element's square root. At last, the complex scattering matrix is given by the sum of the amplitude matrix and the phase.

When the detector aperture is a circle with a diameter D, the point-spread function between the object and the detector is given by

$$\widetilde{h}(x_i,y_i) = \frac{A_R}{\lambda^2 z_i z_0}\Big[2\frac{\mathrm{J}_1(\pi Dr/\lambda z_i)}{\pi Dr/\lambda z_i}\Big]\exp\Big[\mathrm{i}\frac{k}{2z_i}r^2\Big] \times \exp\Big[\mathrm{i}\frac{k}{2z_0}r'^2\Big], \quad (14)$$

where the detector area is $A_R=\pi(D/2)^2$, z_i is the distance between the detector plane and lens, z_o is the distance between the object plane and the detector plane, $\mathrm{J}_1(\cdot)$ is Bessel's function, $r=\sqrt{x_i^2+y_i^2}$ sets the point-spread function $\widetilde{h}(x_i,y_i)$to lie in the center $(m/2,n/2)$ or $[(m+1)/2,(n+1)/2]$.

Figure 5 shows the speckle intensity images of the cone in the case of oblique incident, where the parameters are chosen as: $D=2.5$ cm, $z_0=1$ km, $z_i=f=30$ cm, laser power is 160 W, the beam's waist radius is 10^{-4} m, the surface of the cone is Lambertian, and the BRDF is $1/\pi$.

Figure 6 shows the speckle intensity images of the cone when the laser pulse width is 0.3 ns and wavelength 193 nm. The range of object is 1 m, the speckle size is 300 μm, and the pixel size is 100 μm. In addition, the average effect of the pixel size is not accounted for in the detector.

Figure 6(a) shows that the speckle size increases with increasing wavelength which causes the widening of the impulse response function, where the laser wavelength is 1.06 μm. Figure 6(b) is given when the aperture diameter D is 1.5 cm, which causes the impulse response function to widen as well. In Figs. 6(c) and 6(d), the aperture diameter D is 7.5 cm and 15 cm, separately. As the larger aperture has a smaller speckle size, the speckle image of object is closer to the object.

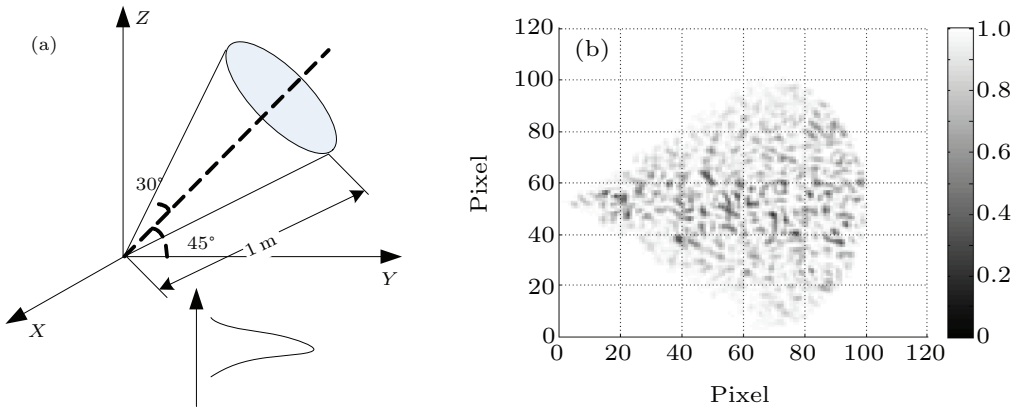


Fig. 5. (a) Direction of irradiating laser beam and (b) speckle intensity images of the cone ($\lambda = 193$ nm, $D = 2.5$ cm).

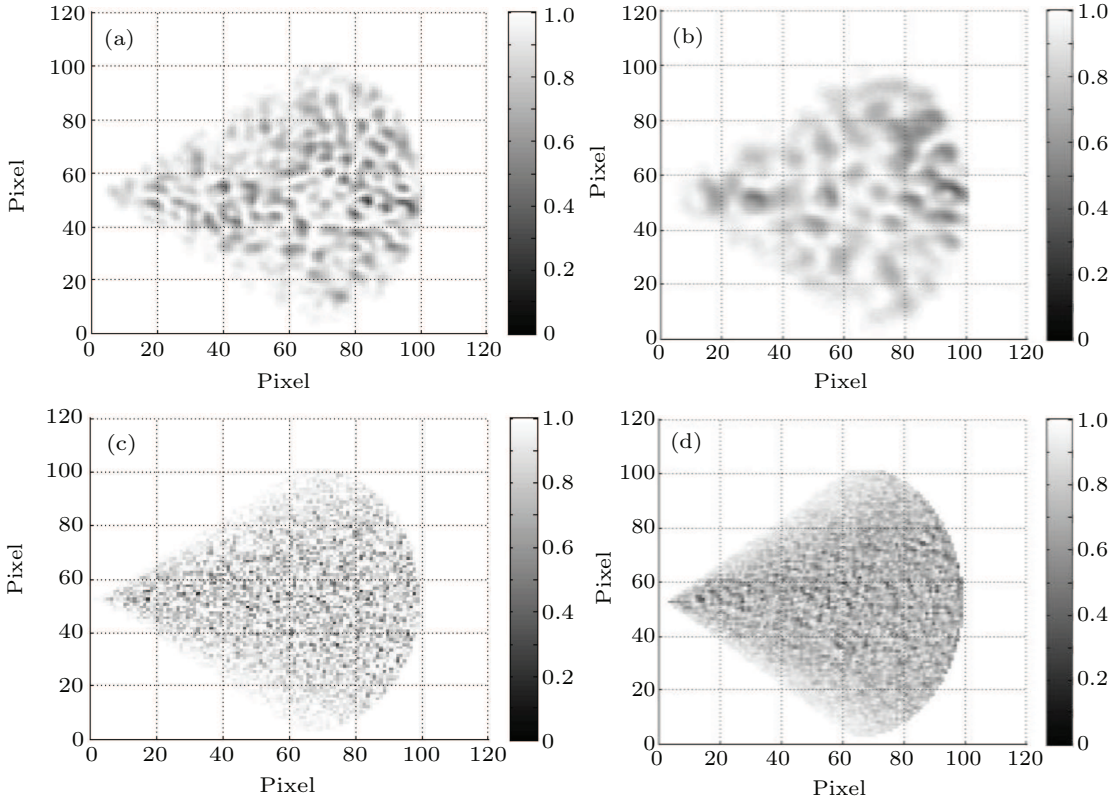


Fig. 6. Effect of aperture size and wavelengths on speckle image of cone. (a) $\lambda = 1.06$ μm, $D = 2.5$ cm; (b) $\lambda = 193$ nm, $D = 1.5$ cm; (c) $\lambda = 193$ nm, $D = 7.5$ cm; (d) $\lambda = 193$ nm, $D = 15$ cm.

5. Experimental results

Figure 7 plots the speckle intensity images of planar object when $L_x = L_y = 2$ cm and $L_x = 2$ cm, $L_y = 1$ cm. The wavelength of the incident laser beam is 0.633 μm, and the distance z between the receive plane and the object plane is 1 m.

To illustrate the information obtained that the longitudinal speckle size gets longer and the transverse basically remains unchanged from Fig. 7(a). That is, the longitudinal speckle size increases with decreasing range of object in the direction.

Figures 8(a) and 8(b) show the speckle image when the distance z is 1.5 m and 5 m respectively, when the size of object is $L_x = L_y = 2$ cm, and the wavelength of the incident laser beam is 0.633 μm. It can be seen that the size of the speckle becomes larger with a longer distance z.

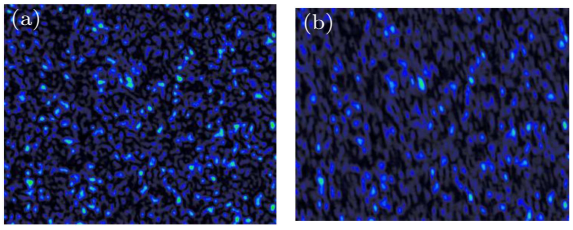


Fig. 7. (color online) Speckle intensity images of planar object (a) $L_x = L_y = 2$ cm; (b) $L_x = 2$ cm, $L_y = 1$ cm.

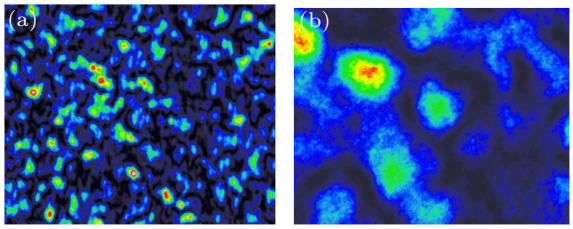


Fig. 8. (color online) Speckle intensity images at different distances. (a) $L_x = L_y = 2$ cm, $z = 1.5$ m; (b) $z = 1.5$ m, $L_x = L_y = 2$ cm, $z = 5$ m.

6. Conclusions

Based on Van Cittert–Zernike theorem, we present the expression of the speckle intensity that is formed on the observation plane with a free-space optical system and the imaging system due to reflection from an area of the object illuminated by a coherent light source. The speckle intensity images of plane target and conical target are obtained by using the Monte Carlo method and experimental measurements, and further presented by varying the characteristics of speckle size with parameters. The results show that the speckle size gets longer with decreasing range extent of target. Instead, with the increase in the distance between the observation plane and the target plane and laser wavelengths, when the receiving aperture is larger and the size of speckle is less, the speckle image of object is closer to the object itself. Therefore, we should choose larger receiving aperture in laser radar system and also we can obtain the information about the size of the scattering object by observing variations of the speckle pattern.

References

[1] David G V, John D G and Paul S I 1991 *Appl. Opt.* **30** 3333
[2] David G V, Keith A. Bush and Paul S Idell 1997 *Appl. Opt.* **36** 1781
[3] Jacob D, Gatt P and Nichols T 2008 *Proc. SPIE* **6950** 69500L
[4] Steinvall O, Sjöqvist L, Henriksson M and Jonsson P 2008 *Proc. SPIE* **6950** 695002
[5] Grnwall C, Steinvall O, Gustafsson F and Chevalier T 2007 *Opt. Eng.* **46** 106
[6] Song H S, Liu M, Liu G Y, Xu Z W, Teng S Y and Cheng C F 2010 *Chin. Phys. B* **19** 074204
[7] Liu W J, Gao R X and Qu S L 2010 *Chin. Phys. B* **19** 024204
[8] Zeng Y G, Wang M Y, Feng G P, Liang X J and Yang G J 2013 *Opt. Lett.* **38** 001313
[9] Feng G P, Chen J B, Lu X L, Han D and Zeng Y G 2013 *Opt. Lett.* **38** 002654
[10] Goodman J 2006 *Speckle Phenomena in Optics: Theory and Applications* (1st edn.) (Colorado: Roberts and Company Publishers) p. 195